

Low & High scale MSSM inflation, gravitational waves and constraints from Planck

Sayantana Choudhury¹, Anupam Mazumdar² and Supratik Pal¹

¹*Physics and Applied Mathematics Unit, Indian Statistical Institute, 203 B.T. Road, Kolkata 700 108, India*

²*Consortium for Fundamental Physics, Physics Department, Lancaster University, LA1 4YB, UK*

(Dated: November 8, 2018)

In this paper we will analyze generic predictions of an *inflection-point* model of inflation with Hubble-induced corrections and study them in light of the *Planck* data. Typically inflection-point models of inflation can be embedded within Minimal Supersymmetric Standard Model (MSSM) where inflation can occur below the Planck scale. The flexibility of the potential allows us to match the observed amplitude of the TT-power spectrum of the cosmic microwave background radiation with low and high multipoles, spectral tilt, and virtually mild running of the spectral tilt, which can put a bound on an upper limit on the tensor-to-scalar ratio, $r \leq 0.12$. Since the inflaton within MSSM carries the Standard Model charges, therefore it is the minimal model of inflation beyond the Standard Model which can reheat the universe with the right thermal degrees of freedom without any *dark-radiation*.

I. INTRODUCTION

The observational success of primordial inflation arising from the cosmic microwave background (CMB) radiation [1, 2] has led to an outstanding question how to embed the inflationary paradigm within a particle theory [3]. Since inflation dilutes all matter except for the quantum vacuum fluctuations of the inflaton, it is pertinent that end of inflation creates all the relevant Standard Model degrees of freedom for the success of Big Bang Nucleosynthesis [4], without any extra relativistic degrees of freedom, i.e. dark radiation [5]¹.

This immediately suggests that the inflationary vacuum cannot be arbitrary and the inflaton must decay *solely* into the Standard Model degrees of freedom. Furthermore, the recent Planck data [5] indicates that the perturbations in the baryons and the cold dark matter are adiabatic in nature, it is evident that there must be a single source of perturbations which is responsible for seeding the fluctuations in all forms of matter².

Strictly speaking this can happen *only* if the inflaton itself carries the Standard Model charges as in the case of Minimal Supersymmetric Standard Model (MSSM) flat-directions [8], where the lightest supersymmetric particle

could be the dark matter candidate and can be created from thermal annihilation of the MSSM degrees of freedom. MSSM inflation was first discussed in Refs. [10–12], and in recently, see Refs. [13–18]. The inflaton candidates are made up of *gauge invariant* combinations of squarks (supersymmetric partners of quarks) and sleptons (supersymmetric partners of leptons).

One of the *key* ingredients for embedding inflation within MSSM is that the inflaton VEV must be below the Planck scale, $M_{PL} = 2.4 \times 10^{18}$ GeV. This justifies the application of an effective field theory treatment at low energies. It is well-known that the potential for the MSSM flat-direction inflaton has high degree of *flexibility* – the potential can accommodate *inflection-point* below the Planck VEV, which allows a rich class of flat potentials, with a vanishing effective mass, which has been studied analytically and numerically [11, 19, 20]. The application of inflection point inflation is not just limited to particle theory, but such potentials have also found their applications in string theory [21].

It has also been known that inflection-point models of inflation can occur for a wide range of Hubble values, H_{inf} , ranging from 10^{-1} GeV $< H_{inf} \leq 10^{13}$ GeV. For very high scale inflation there is a possibility of obtaining signatures for the primordial gravitational waves, namely the B-modes [22] below the Planck scale³.

The aim of this paper is to show explicitly how large scale inflection-point inflation can match the current CMB observables, namely the TT-part of the temperature anisotropy spectrum, low and high multipoles, spectral tilt, running of the spectral tilt, and running of the spectral tilt. We will also provide the ranges of tensor-to-scalar ratio r , which is compatible with all

¹ Embedding the last 50 -60 e-foldings of inflation within string theory has a major disadvantage. Due to large number of hidden sectors arising from any string compactifications, it is likely that the inflaton energy density will get dumped into the hidden sectors instead of the visible sector [6]. The branching ratio for the inflaton decay into the visible sector is very tiny, therefore reheating the Standard Model degrees of freedom is one of the biggest challenges for any string motivated models of inflation. Furthermore, many of the compactifications generically lead to extra dark radiation (massless axions) which are already at the verge of being ruled out by the present data [7].

² In principle more than one fields can still participate during inflation, but they must do so in such a way that here exists an attractor solution which would yield solely adiabatic perturbations and no isocurvature perturbations, such as in the case of assisted inflation [9].

³ We are assuming that the gravitational modes can be quantized with quantum initial conditions. If the gravity waves behave classically, then the amplitude of the gravitational waves in a simple scalar field driven model will be absolutely zero [23], as there is no source term for the gravitational waves.

the data sets ⁴.

In section II, we will discuss the generality of inflection-point potential. In section II A, we will provide a brief discussion on supergravity corrections, and the two regimes of inflation will be discussed in section III. In section IV, we will discuss the cosmological observables relevant for CMB, in section V, we will discuss reheat temperature and the number of e-foldings. In section VI, we will discuss tensor-to-scalar ratio of high and low scale models of inflation. In section VII, we will provide the TT-power spectrum (low and high multipoles) for a particular realisation, and in section VIII, we will conclude our results.

II. FLAT POTENTIAL AROUND THE INFLECTION-POINT

The most generic inflection-point potential can be recast as [20, 22]:

$$V(\phi) = \alpha + \beta(\phi - \phi_0) + \gamma(\phi - \phi_0)^3 + \kappa(\phi - \phi_0)^4 + \dots, \quad (1)$$

where any generic potential, $V(\phi)$, has been expanded around the inflection-point, ϕ_0 , where α denotes the cosmological constant, and coefficients β , γ , κ determine the shape of the potential in terms of the model parameters. Typically, α can be set to zero by fine tuning, but here we wish to keep this term for generality. Note that not all of the coefficients are independent once we prescribe inflaton within MSSM.

In Refs. [10, 11, 13, 28, 29] the authors have recognized two D -flat directions which can be the ideal inflaton candidates. Both $\tilde{u}\tilde{d}\tilde{d}$, where \tilde{u} , \tilde{d} correspond to the right handed squarks, and $\tilde{L}\tilde{L}\tilde{e}$, where \tilde{L} is the left handed slepton, and \tilde{e} is the right handed (charged) leptons, flat directions are lifted by higher order superpotential terms of the following simple form:

$$W(\Phi) = \frac{\lambda}{6} \frac{\Phi^6}{M_{PL}^3}, \quad (2)$$

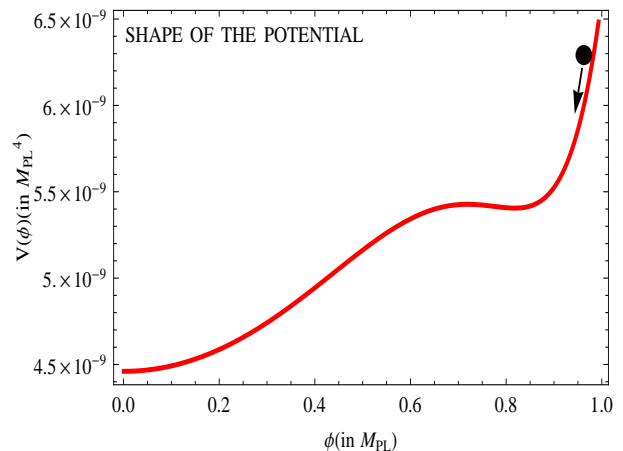
where $\lambda \sim \mathcal{O}(1)$ coefficient. The scalar component of Φ superfield, denoted by ϕ , is given by

$$\phi = \frac{\tilde{u} + \tilde{d} + \tilde{d}}{\sqrt{3}}, \quad \phi = \frac{\tilde{L} + \tilde{L} + \tilde{e}}{\sqrt{3}}, \quad (3)$$

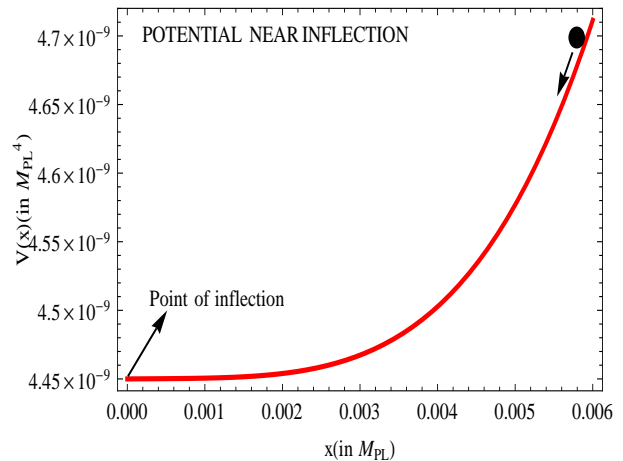
for the $\tilde{u}\tilde{d}\tilde{d}$ and $\tilde{L}\tilde{L}\tilde{e}$ flat directions, respectively.

A. Brief discussion on Hubble induced corrections

In addition to Eq. (2), there are many possible contributions to the vacuum energy. It is conceivable that



(a) Shape of the potential. Note the existence of a flat plateau below the Planck scale.



(b) The blow up picture of the potential near the inflection point. Here $x = \phi - \phi_0$, where ϕ_0 is the inflection-point.

FIG. 1: Inflationary potential including Hubble induced corrections.

at high energies the universe is dominated by a large cosmological constant arising from a string theory landscape [30]. Our own patch of the universe could be locked in a false vacuum within an MSSM landscape [31], or there could be hidden sector contributions [32, 33], or there could be a combination of these effects. For simplicity we may attribute such a vacuum energy to a hidden sector. A hybrid model of inflation [24] also provides a source of vacuum energy density during inflation. For the purpose of illustration, we will model earlier phases of inflation driven by the superpotential of type:

$$W(S) = M^2 S, \quad (4)$$

where M is some high scale which dictates the initial vacuum energy density, and S is the hidden sector superfield. The total Kähler potential can be of the form [34–36]:

$$K = S^\dagger S + \Phi^\dagger \Phi + \delta K, \quad (5)$$

⁴ Similar studies were undertaken for hybrid inflation model [24, 25], after the *Planck* data release, see [26]. For power law inflation, see [27].

where the non-minimal term δK can be any of these functional forms:

$$\delta K = f(\Phi^\dagger\Phi, S^\dagger S), f(S^\dagger\Phi\Phi), f(S^\dagger S^\dagger\Phi\Phi), f(S\Phi^\dagger\Phi)$$

We will always treat the fields $s, \phi \ll M_{PL}$. The higher order corrections to the Kähler potential are extremely hard to compute. It has been done within a string theory setup [37] but only in very special circumstances, and not for MSSM fields. The scalar potential in $\mathcal{N} = 1$ supergravity can be written in terms of superpotential, W , and Kähler potential, K , as

$$V = e^{K(\Phi, \Phi^\dagger)/M_{PL}^2} \left[(D_{\Phi_i} W(\Phi)) K^{\Phi_i \bar{\Phi}_j} (D_{\bar{\Phi}_j} W^*(\Phi^\dagger)) - \frac{3}{M_{PL}^2} |W(\Phi)|^2 \right] + (\text{D-terms}), \quad (6)$$

where $F_\Phi \equiv D_\Phi W = W_\Phi + K_\Phi W/M_{PL}^2$, and $K^{\Phi_i \bar{\Phi}_j}$ is the inverse matrix of $K_{\Phi_i \bar{\Phi}_j}$, and the subscript denotes derivative with respect to the field. Hereafter, we neglect the contribution from the D-term, since the MSSM inflatons are D-flat directions. In the above potential $W = W(S) + W(\Phi)$.

After minimizing the potential along the angular direction, θ ($\Phi = \phi e^{i\theta}$), we take the real part of ϕ by rotating it to the corresponding angle θ , resulting in [34–36]:

$$V(\phi, \theta) = V_0 + \frac{(m_\phi^2 + c_H H^2)}{2} |\phi|^2 + (a_H H + a_\lambda m_\phi) \frac{\lambda \phi^6}{6M_{PL}^3} \cos(6\theta + \theta_{a_H} + \theta_{a_\lambda}) + \frac{\lambda^2 |\phi|^{10}}{M_{PL}^6} \quad (7)$$

where the cosmological constant will be determined by the overall inflationary potential, $V_0 \approx 3H^2 M_{PL}^2$. Usually this bare cosmological term can be set to zero from the beginning by tuning the graviton mass. We will consider scenarios, where we will have $V_0 \neq 0$ and $V_0 = 0$.

Note that m_ϕ and a_λ are soft-breaking mass and the non-renormalizable A -term respectively (A is a positive quantity since its phase is absorbed by a redefinition of θ during the process)⁵. The potential also obtains Hubble-induced corrections, with coefficients $c_H, a_H \sim \mathcal{O}(1)$. Their exact numerical values will depend on the nature of Kähler corrections and compactification, which are hard to compute for a generic scenario [37], but the corrections typically yield $\sim \mathcal{O}(1)$ coefficients. The non-renormalizable terms have a periodicity of 2π in (ϕ, θ) 2D plane, $\theta_{a_H}, \theta_{a_\lambda}$ are the extra phase factors.

⁵ The masses are given by:

$$m_\phi^2 = \frac{m_L^2 + m_L^2 + m_\tilde{e}^2}{3}, \quad m_\phi^2 = \frac{m_u^2 + m_d^2 + m_d^2}{3}$$

for $\tilde{L}\tilde{L}\tilde{e}$ and $\tilde{u}\tilde{d}\tilde{d}$ directions respectively. Typically these masses are set by the scale of supersymmetry, in the low scale case the masses will be typically of order $\mathcal{O}(1)$ TeV.

III. TWO REGIMES OF INFLATION: LOW & HIGH

There are two regimes where one can describe the dynamics of the potential:

A. $m_\phi \gg H$: Low scale inflation

Since $c_H, a_H \sim \mathcal{O}(1)$ the Hubble-induced terms do not play any crucial role in this case, and the scale of inflation remains very low. As a result the tensor-to-scalar ratio, r , becomes too small to be ever detectable. This was the scenario studied in Refs. [10, 11]. In this case we can set its value to $V_0 = 0$ from the beginning by tuning the gravitino mass [38]. The potential can be minimized along the θ direction, which reduces to [10, 11]:

$$V(\phi, \theta) = \frac{m_\phi^2}{2} |\phi|^2 - a_\lambda m_\phi \frac{\lambda \phi^6}{6M_{PL}^3} + \frac{\lambda^2 |\phi|^{10}}{M_{PL}^6} \quad (8)$$

For,

$$\frac{a_\lambda^2}{40} \equiv 1 - 4\delta^2, \quad (9)$$

and $\delta^2 \ll 1$, there exists a point of inflection (ϕ_0) in $V(\phi)$, where

$$\phi_0 = \left(\frac{m_\phi M_{PL}^3}{\lambda \sqrt{10}} \right)^{1/4} + \mathcal{O}(\delta^2), \quad (10)$$

$$V''(\phi_0) = 0, \quad (11)$$

at which

$$\alpha = V(\phi_0) = \frac{4}{15} m_\phi^2 \phi_0^2 + \mathcal{O}(\delta^2), \quad (12)$$

$$\beta = V'(\phi_0) = 4\alpha^2 m_\phi^2 \phi_0 + \mathcal{O}(\delta^4), \quad (13)$$

$$\gamma = V'''(\phi_0) = 32 \frac{m_\phi^2}{\phi_0} + \mathcal{O}(\delta^2). \quad (14)$$

The potential is specified completely by m_ϕ and λ . However m_ϕ is determined by the soft-SUSY breaking mass parameter, which is well constrained by the current ATLAS [39] and CMS [40] data, and we shall take $m_\phi = 1$ TeV. For $m_\phi \sim 1$ TeV, $H^* \sim 0.1$ GeV, and our assumption of neglecting H in such a case is well justified. We will always consider $\lambda = 1$ in our analysis.

B. $H \gg m_\phi$: High scale inflation

The supergravity corrections become important, the Hubble-induced terms dominate the potential. This can happen quite naturally if there exists a previous source of effective cosmological constant term described in Refs. [14, 22]. In this case one can safely ignore the

soft SUSY breaking mass term, and since $a_\lambda \sim \mathcal{O}(1)$, one can safely consider only the Hubble-induced non-renormalizable term. One advantage of considering such a potential is to obtain large tensor-to-scalar ratio, r , which can be within the range of Planck and other future CMB B-mode polarization experiments. We will keep V_0 in this case, and the potential simplifies to [14]:

$$V(\phi) = V_0 + \frac{c_H H^2}{2} |\phi|^2 - \frac{a_H H \phi^6}{6M_{PL}^3} + \frac{|\phi|^{10}}{M_{PL}^6}. \quad (15)$$

where we have taken $\lambda = 1$. The potential admits inflection point for $a_H^2 \approx 40c_H^2$. We characterize the required fine-tuning by the quantity, δ , defined as [11]

$$\frac{a_H^2}{40c_H^2} = 1 - 4\delta^2. \quad (16)$$

When $|\delta|$ is small, a point of inflection ϕ_0 exists such that $V'''(\phi_0) = 0$, with

$$\phi_0 = \left(\sqrt{\frac{c_H}{10}} H M_{PL}^3 \right)^{1/4}. \quad (17)$$

For $\delta < 1$, we can Taylor-expand the inflaton potential around the inflection point $\phi = \phi_0$ similar to Eq. (1), where the coefficients are now given by:

$$\alpha = V(\phi_0) = V_0 + \left(\frac{4}{15} + \frac{4}{3}\delta^2 \right) c_H H^2 \phi_0^2 + \mathcal{O}(\delta^4), \quad (18)$$

$$\beta = V'(\phi_0) = 4\delta^2 c_H H^2 \phi_0 + \mathcal{O}(\delta^4), \quad (19)$$

$$\gamma = \frac{V''(\phi_0)}{2!} = \frac{c_H H^2}{\phi_0} (32 - 80\delta^2) + \mathcal{O}(\delta^4), \quad (20)$$

$$\kappa = \frac{V''''(\phi_0)}{4!} = \frac{c_H H^2}{\phi_0^2} (384 - 1260\delta^2) + \mathcal{O}(\delta^4). \quad (21)$$

Note that once we specify c_H and H , all the terms in the potential are determined. In this regard the potential indeed simplifies a lot to study the cosmological observables. In section VII, we will be scanning over c_H , H to obtain the best fits with the current observations.

One must also ensure that the vacuum energy density which generated the large cosmological constant in the first place vanishes by the end of slow-roll inflation. This typically happens in the case of hybrid inflation [24, 25], and as discussed in [20, 22, 49]. In the string landscape [30], or in the case of MSSM [31], this can happen through bubble nucleation, provided the rate of nucleation is such that $\Gamma_{nucl} \gg H$. In the latter case all the bubbles will belong to the MSSM vacuum—similar to the first order phase transition in the electroweak symmetry breaking scenario. However, one has to make sure that the cosmological constant disappears in the MSSM vacuum right at the end of inflation [58].

IV. CMB OBSERVABLES AND INFLECTION POINT

In this section our primary focus is to study the cosmological observables to match the CMB data for an inflection-point inflation whose potential is given by Eq. (15). First we use the following parameterizations for the amplitude of the scalar perturbations, P_S , tensor perturbations, P_T , and the tensor-to-scalar ratio r , in terms of the slow-roll parameters [41, 42]:

$$P_S(k) = P_S(k_*) \left(\frac{k}{k_*} \right)^{n_S - 1 + \frac{\alpha_S}{2} \ln\left(\frac{k}{k_*}\right) + \frac{\kappa_S}{6} \ln^2\left(\frac{k}{k_*}\right) + \dots}, \quad (22)$$

$$P_T(k) = P_T(k_*) \left(\frac{k}{k_*} \right)^{n_T + \frac{\alpha_T}{2} \ln\left(\frac{k}{k_*}\right) + \frac{\kappa_T}{6} \ln^2\left(\frac{k}{k_*}\right) + \dots}, \quad (23)$$

$$r(k) = \frac{P_T(k)}{P_S(k)} = r(k_*) \left(\frac{k}{k_*} \right)^{n_T - n_S + 1 + \frac{(\alpha_T - \alpha_S)}{2} \ln\left(\frac{k}{k_*}\right) + \frac{(\kappa_T - \kappa_S)}{6} \ln^2\left(\frac{k}{k_*}\right) + \dots} \quad (24)$$

where the observables are now given in terms of the inflationary potential, running of the spectral tilt α_S , α_T , and running of the running, given by κ_S , κ_T , where the subscripts S and T denote scalar and tensor modes. Here the consistency relations are modified at the second order due to the presence of running. The above parametrization are realized by expanding the scale dependent slow-

roll parameters around the pivot scale $k = k_*$ and they have been listed in an appendix (see Eqs. (32,33)).

Cosmological parameter estimation can be done more precisely once we allow the higher order radiative corrections to the slow-roll parameters [43]. We have listed all the relevant cosmological observables in an appendix (see Eqs. (34)-(41)). In our case we have obtained the pre-

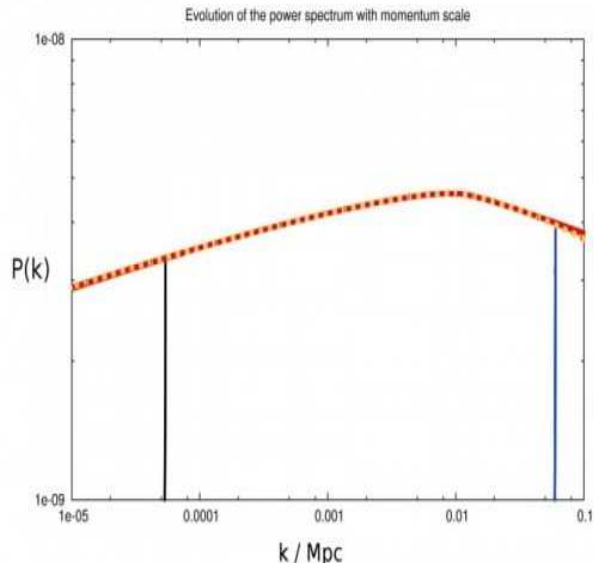


FIG. 2: We show the evolution of the power spectrum, $P(k)$, for high scale model of inflation when $H \gg m_\phi$. The specific values of the model parameters are: $\delta \sim 10^{-4}$ (see Eq. (16)), $\lambda = 1$, $c_H = 2$, $a_H = 2.108$, $\phi_0 = 1.129 \times 10^{16}$ GeV for the entire range of momentum, k , that crosses the Hubble patch during the 17 e-folds of inflation. Here the *orange* dotted curve is obtained from the higher order radiative corrections to the slow-roll parameters, see appendix Eq. (34), and the *red* curve from numerically integrating the cosmological perturbations. The *blue* vertical line corresponds to $k_{max} = 0.056 \text{ Mpc}^{-1}$ for $l_{max} = 2500$, which is the highest probing limit of recent *Planck* data. On the other hand the *black* vertical line corresponds to $k_{min} = 4.488 \times 10^{-5} \text{ Mpc}^{-1}$ for $l_{min} = 2$.

dicted power spectrum from the higher order radiative corrections to the slow-roll parameters, and also numerically we have evolved the perturbations which we will discuss below.

In order to illustrate this, let us consider the case when $H \gg m_\phi$. In this case there is a possibility of detecting large tensor-scalar ratio, r . We start our analysis numerically by using cosmological code CAMB [44] with the well known Bunch-Davies in-in vacuum state [45], and also perform the quantum fluctuations via cosmological linear perturbation theory, see Ref. [41, 46]. In figure 2, we have shown the evolution of the power spectrum for the entire range of momentum scale across the 17 e-folds of inflation which has been observed by the *Planck* satellite [1, 47]. In this plot the *orange* dotted curve is obtained from the radiative corrections to the higher order slow-roll corrections. On the other hand the *red* curve is the outcome of our numerical analysis. As we can see that the higher order radiative corrections to the slow-roll parameters is quite a good approximation when compared to the results obtained from the numerical analysis for the observed range of $k_{max} = l_{max}/\eta_0\pi \sim \mathcal{O}(0.056 \text{ Mpc}^{-1})$ for $l_{max} = 2500$ down to $k_{min} \sim \mathcal{O}(10^{-5} \text{ Mpc}^{-1})$ for $l_{min} = 2$, where $\eta_0 \sim 14000 \text{ Mpc}$ is the conformal time at

present epoch [1, 47]. The slow roll approximations differ very minutely from the numerical estimation, but for very large values of k , or very small wavelength regimes beyond $l \gg 2500$.

V. ESTIMATION OF REHEAT TEMPERATURE AND THE SCALE OF INFLATION

We need to compute the pivot scale, k_* , when the relevant perturbations had left the Hubble patch during inflation. We can compute by expressing the number of e-foldings during inflation, which is given by [1, 48, 49]:

$$N_* \approx 71.21 - \ln\left(\frac{k_*}{k_0}\right) + \frac{1}{4} \ln\left(\frac{V_*}{M_P^4}\right) + \frac{1}{4} \ln\left(\frac{V_*}{\rho_{end}}\right) + \frac{1 - 3w_{int}}{12(1 + w_{int})} \ln\left(\frac{\rho_{rh}}{\rho_{end}}\right), \quad (25)$$

where ρ_{end} is the energy density at the end of inflation, ρ_{rh} is an energy scale during reheating, $k_0 = a_0 H_0$ is the present Hubble scale, V_* corresponds to the potential energy when the relevant modes left the Hubble patch during inflation and w_{int} characterizes the effective equation of state parameter between the end of inflation and the energy scale during reheating. For our model we have $w_{int} = 1/3$ exactly for which the contribution from the last term in Eq. (25) vanishes. For inflation driven by the MSSM flat directions the time scale for the transfer of energy to the MSSM relativistic species can be computed exactly as in [50]. This happens roughly within one Hubble time. This is due to the gauge couplings of the inflaton to gauge/gaugino fields. Within 10 – 20 inflaton oscillations radiation-dominated universe prevails, as shown in Ref. [50]. The resultant *upper-bound* on the reheat temperature at which all the MSSM *degrees of freedom* are in thermal equilibrium (kinetic and chemical equilibrium) is given by [50]

$$T_{rh} = \left(\frac{30}{\pi^2 g_*}\right)^{\frac{1}{4}} \sqrt[4]{V_*} \leq 6.654 \times 10^{15} \sqrt[4]{\frac{r_*}{0.12}} \text{ GeV}. \quad (26)$$

where we have used $g_* = 228.75$ (all the degrees of freedom in MSSM). Since the temperature of the universe is so high, the lightest supersymmetric particle (LSP) relic density is then given by the standard (thermal) *freeze-out* mechanism [51]. In particular, if the neutralino is the LSP, then its relic density is determined by its annihilation and coannihilation rates [28, 29, 52]. The advantage of realizing inflation in the visible sector is that it is possible to nail down the thermal history of the universe precisely. At temperatures below 100 GeV there will be no extra degrees of freedom in the thermal bath except that of the SM, therefore BBN can proceed without any trouble.

For low scale models of inflation, i.e. $m_\phi \gg H$, the tensor modes are utterly negligible. For $m_\phi \sim 1 \text{ TeV}$, and $\phi_0 \sim 3 \times 10^{14} \text{ GeV}$, the value of $H_* \sim 10^{-1} \text{ GeV}$,

see Eq.(10). The estimation of the reheat temperature is given by the equality of the above Eq. (26). The reheat temperature is typically 3×10^8 GeV for the above parameters. Note that for $m_\phi \gg H$, the tensor to scalar ratio r does not scale with the reheat temperature.

Note that saturating the upper-bound on $r \sim 0.12$ would yield a large reheating temperature of the universe. It is sufficiently large to create gravitino from a thermal bath [53, 54]. The gravitino production from the direct decay of the inflaton will be suppressed [55]. In this case, the gravitino abundance is compatible with the BBN bounds, provided the gravitino mass, $m_{3/2} \geq \mathcal{O}(10)$ TeV, see [56]. The bound holds only for a decaying gravitino, for which the graviton will decay before the BBN. If gravitino happens to be the LSP, then such a high scale model of inflation with large Hubble-induced corrections will be ruled out, unless there is some late entropy injection or there are some kinematical reasons for which the gravitino production is highly suppressed [57].

VI. TENSOR TO SCALAR RATIO FOR HIGH & LOW SCALE MODELS OF INFLATION

The Planck constraint implies that the tensor-to-scalar ratio, r , at the pivot scale $k = k_*$, corresponds to an upper bound on the energy scale of the Hubble induced inflection point inflation:

$$V_* \leq \frac{3}{2}\pi^2 P_S(k_*) r_* M_{PL}^4 = (1.96 \times 10^{16} \text{ GeV})^4 \frac{r_*}{0.12}. \quad (27)$$

For an example, at the pivot scale $k_* = 0.002 \text{ Mpc}^{-1}$, the corresponding upper bound on the energy density becomes $V_* = 1.89 \times 10^{16} \text{ GeV}$. The equivalent statement can be made in terms of the upper bound on the numerical value of the Hubble parameter during inflation as

$$H_* \leq 9.241 \times 10^{13} \sqrt{\frac{r_*}{0.12}} \text{ GeV}. \quad (28)$$

Here in eqn (26), eqn (27) and eqn (28) the equalities hold good in high scale inflationary regime ($H \gg m_\phi$). The inequalities are more significant once we enter low scale inflationary ($m_\phi \gg H$) region.

We scan the model parameters for obtaining large tensor to scalar ratio, r , for the following values:

$$\begin{aligned} c_H &\sim \mathcal{O}(1 - 10), \\ a_H &\sim \mathcal{O}(10 - 100), \\ \lambda &\sim \mathcal{O}(1), \\ \phi_0 &\sim \mathcal{O}((1 - 3) \times 10^{16} \text{ GeV}) \end{aligned} \quad (29)$$

Now including the higher order corrections to the slow-roll parameters, the inflationary observables are esti-

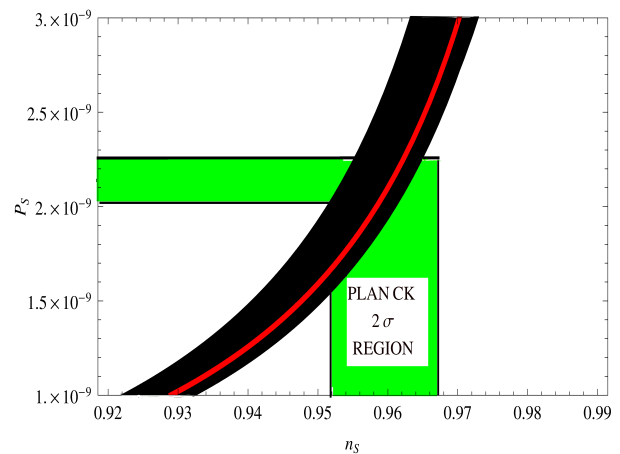


FIG. 3: For large scale inflation, $H \gg m_\phi$, we have shown the variation of P_S vs n_s . The red curve shows the model parameters, $\delta \sim 10^{-4}$, $\lambda = 1$, $c_H = 2$, $a_H = 2.108$, $\phi_0 = 1.129 \times 10^{16} \text{ GeV}$, for the pivot scale $k_* = 0.002 \text{ Mpc}^{-1}$. The green shaded region shows the 2σ CL. range in n_s allowed by the Planck data [1]. Instead of getting a single solid red curve we get a black shaded region if we consider the full parameter space for high scale ($H \gg m_\phi$) inflation given by Eq. (29).

mated from our model as following:

$$\begin{aligned} 2.092 &< 10^9 P_S < 2.297, \\ 0.958 &< n_s < 0.963, \\ r &< 0.12, \\ -0.0098 &< \alpha_S < 0.0003, \\ -0.0007 &< \kappa_S < 0.006 \end{aligned} \quad (30)$$

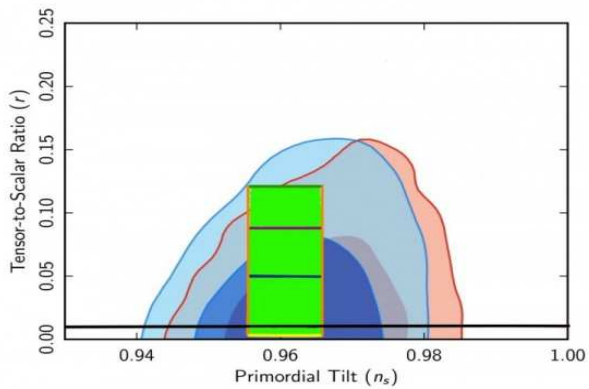
which confronts the *Planck*+WMAP-9+BAO data set, [1, 5, 47, 59], well within 2σ CL. Furthermore, we consider the following values of the model parameters which match the TT-spectrum of the CMB data for high scale model of inflation, i.e. $H \gg m_\phi$,

$$\begin{aligned} \delta &\sim 10^{-4}, \quad \lambda = 1, \quad c_H = 2, \quad a_H = 12.650, \\ \phi_0 &= 1.129 \times 10^{16} \text{ GeV} = 4.704 \times 10^{-3} M_{PL}. \end{aligned} \quad (31)$$

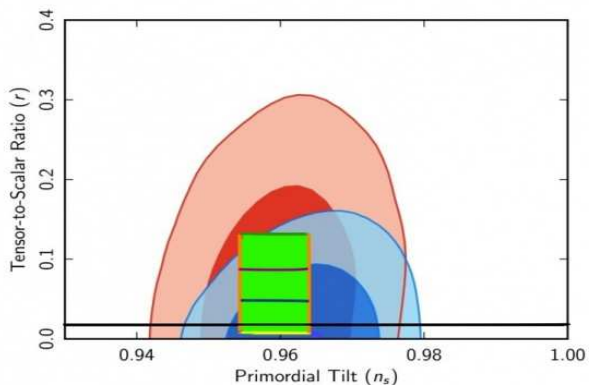
Using Eq. (31), in Fig. (3) we have shown the behavior of the amplitude of the the power spectrum, P_S with respect to spectral tilt, n_s at the pivot scale $k_* = 0.002 \text{ Mpc}^{-1}$ by a red curve. If we take care of the full parameter space, see Eq. (29), there are solutions which have been shown in a black shaded region.

In principle, we can vary H_* from high scales to low scales. Since in our case the advantage is that the thermal history is well established, we can trace the relevant number of e-foldings, i.e. N_* for various ranges of H_* . By varying $10^{-1} \text{ GeV} < H_* \leq 9.241 \times 10^{13} \text{ GeV}$, we can probe tensor-to-scalar ratio for a wide range: $10^{-29} < r_* \leq 0.12$.

Furthermore, by using *Planck*+WMAP-9 and *Planck*+WMAP-9+BAO datasets with Λ CDM background along with different combined constraints, we



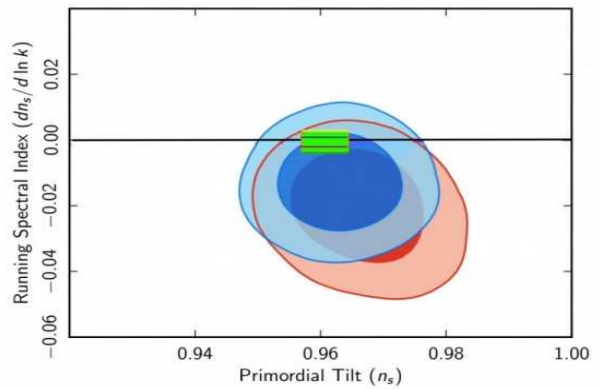
(a) r vs n_S . By varying H_* we can probe a wide range of tensor-to-scalar ratio: $10^{-29} < r_* \leq 0.12$. The vertical line on the left corresponds to $N = 50$, while the right line corresponds to $N = 70$.



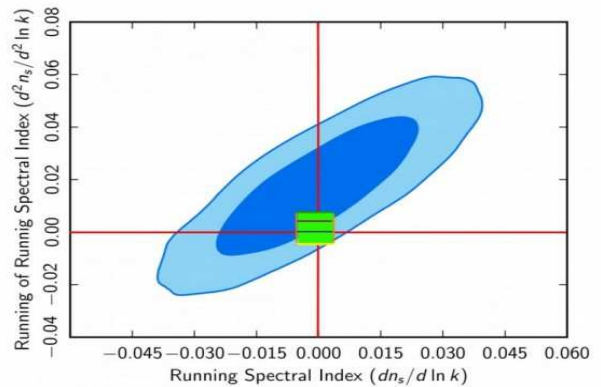
(b) r vs n_S . By varying H_* we can probe a wide range of tensor-to-scalar ratio: $10^{-29} < r_* \leq 0.12$. The vertical line on the left corresponds to $N = 50$, while the right line corresponds to $N = 70$.

FIG. 4: We show the joint 1σ and 2σ CL. contours using (a) Planck+WMAP-9 data with Λ CDM+r(Blue region), and Λ CDM+r + α_S (Red region), (b) Planck+WMAP-9+BAO data with Λ CDM+r(Blue region) and Λ CDM+r + α_S (Red region). The straight lines parallel to n_S axis are drawn by varying the Hubble parameter H_* within the range $10^{-1} \text{ GeV} < H_* \leq 9.241 \times 10^{13} \text{ GeV}$. The deep green line and the yellow line correspond to the upper and lower bound of H_* respectively. The green shaded region bounded by orange lines represent the allowed region obtained from the model. Additionally, the black thick line divides the low scale ($m_\phi \gg H$) and the high scale ($H \gg m_\phi$) regions of inflation.

have shown the status of inflection point inflationary model in the marginalized 1σ and 2σ CL. contours in Fig. (4). The allowed region from the model is explicitly shown by the green shaded region bounded by orange vertical lines parallel to r -axis. Along the vertical lines the number of e-foldings varies within $50 < N_* < 70$ (from left to right) for various ranges of H_* as mentioned earlier. We have also shown a thick black line parallel to n_S axis in Fig. (4) which discriminates between the low scale ($m_\phi \geq H$) and high scale ($H \gg m_\phi$)



(a) α_S vs n_S



(b) κ_S vs α_S

FIG. 5: We show the joint 1σ and 2σ CL. contours using Planck+WMAP-9+BAO with (a) Λ CDM+ α_S (Blue region) and Λ CDM+ α_S + r (Red region), (b) Λ CDM+ α_S + κ_S (Blue region) background. The straight lines parallel to n_S axis are drawn by varying the Hubble parameter H_* within the range $10^{-1} \text{ GeV} < H_* \leq 9.241 \times 10^{13} \text{ GeV}$. The deep green line and the yellow line correspond to the upper and lower bound of H_* respectively. The green shaded region bounded by orange lines represent the allowed region obtained from the model.

inflationary scenarios. Additionally, we have depicted various straight lines for the intermediate values of H_* within the allowed region. The model also provides very mild running, α_s , and running of running, κ_S , which is also shown in the marginalized 1σ and 2σ CL. contours in Fig. (5), where we have used Planck+WMAP-9 and Planck+WMAP-9+BAO datasets with Λ CDM background along with different combined observational constraints.

VII. MULTIPOLE SCANNING OF TT-SPECTRA AND CMB ANISOTROPY

In this section we study the TT-angular power spectrum for the CMB anisotropy. For our present setup at low ℓ region ($2 < l < 49$) the contributions from the

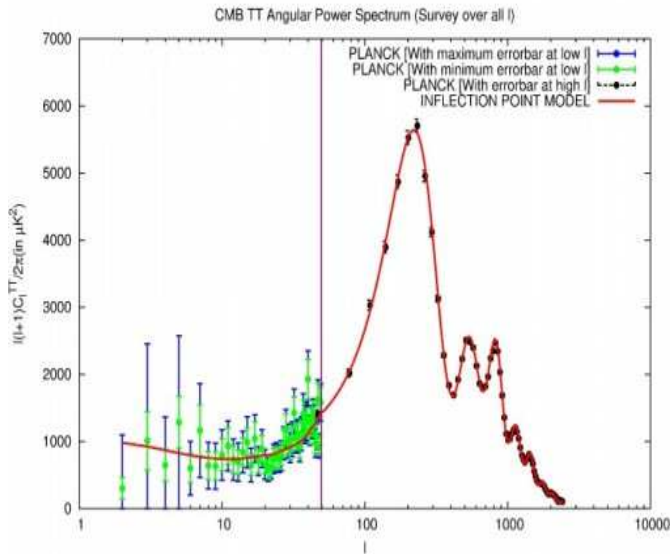


FIG. 6: TT-power spectrum for ℓ ($2 < \ell < 2500$). The vertical line is drawn at $l = 50$ which separates the low- l ($2 < l < 50$) and high- l ($50 < l < 2500$) region. Here the TT-power spectrum is drawn for the parameter values mentioned in Eq. (31) in the context of high scale ($H \gg m_\phi$) Hubble induced inflationary framework.

running (α_S, α_T), and running of running (κ_S, κ_T) are very small. Consequently their additional contribution to the power spectrum for scalar and tensor modes becomes unity ($\sim \mathcal{O}(1)$) (this is consistent with the initial condition at the pivot scale $k = k_*$) and the original power spectrum becomes unchanged. As a result the proposed model will be well fitted with the *Planck* low- l data within high cosmic variance except for a few outliers. On the other hand, when we move towards high ℓ regime ($50 < l < 2500$) the contribution of running and running of running become stronger and this will enhance the power spectrum to a permissible value such that it will accurately fit *Planck* high- l data within very small cosmic variance. In this way one can easily survey over all the multipoles starting from low- l to high- l using the same parameterizations as mentioned in Eqs. (31).

From Figs. (6), we see that the Sachs-Wolfe plateau obtained from our model is non flat, confirming the appearance of running, and running of the running in the spectrum observed for low l region ($l < 50$). For larger value of the multipole ($50 < l < 2500$), CMB anisotropy spectrum is dominated by the Baryon Acoustic Oscillations (BAO), giving rise to several ups and downs in the spectrum, see [60]. Note that high l regions of our model are well fitted within the small cosmic variance observed by *Planck*. In the low l region due to the presence of very large cosmic variance there may be other pre-inflationary

scenarios which might be able to fit the TT-power spectrum better [47]. In our study we have considered only the possibility for which the model is well fitted for both low and high l regions.

VIII. CONCLUSION

In this paper we have considered a simple model of inflection-point inflation motivated by the MSSM flat directions, where we have taken potentials with both supergravity corrections are important and negligible. In the former case, we yield significantly large tensor-to-scalar ratio, $r \leq 0.12$, for $H_* \sim 9.24 \times 10^{13}$ GeV and the VEV $\phi_0 = 1.12 \times 10^{16}$ GeV. The model fits the amplitude of the power spectrum and the spectral tilt. The model predicts mild running and running of the running of the spectral tilt well within the 2σ uncertainties. In particular, the high scale inflection-point inflation model fits the high l multipoles of the *Planck* data quite well with the Λ CDM parameters. The low l multipoles have high uncertainties and they are within the cosmic variance. The forthcoming polarization data from *Planck* will hopefully further constrain the inflection-point model of inflation. The model tends to predict a perfect match for the spectral tilt even for a small tensor-to-scalar ratio, r , as seen in Fig. (4).

The perturbations created from the slow roll evolution of the inflaton are Gaussian and adiabatic. The amplitude and the spectral tilt match very well with the *Planck* data. One of the advantages of the proposed model is that it is embedded fully within MSSM, and therefore it predicts the right thermal history of the universe with *no extra relativistic degrees of freedom* other than that of the Standard Model.

Acknowledgments

AM would like to thank Pratika Dayal and Seshadri Nadathur for helpful discussions. SC thanks Council of Scientific and Industrial Research, India for financial support through Senior Research Fellowship (Grant No. 09/093(0132)/2010). SC also thanks Arnab Dasgupta for useful suggestions. AM is supported by the Lancaster-Manchester-Sheffield Consortium for Fundamental Physics under STFC grant ST/J000418/1. SP thanks ISI Kolkata for computational support through a research grant.

Appendix

The power spectrums as well as other relevant parameters in terms of the potential can be written as [41, 42]:

$$\begin{aligned}
\epsilon_V(k) &= \epsilon_V - \frac{\alpha_T}{2} \ln\left(\frac{k}{k_*}\right) + \frac{\kappa_T}{4} \ln^2\left(\frac{k}{k_*}\right) + \dots, \\
\eta_V(k) &= \eta_V - \frac{(\alpha_S - 3\alpha_T)}{2} \ln\left(\frac{k}{k_*}\right) + \frac{1}{2} \left(\kappa_S - 3\kappa_T + \{n_T^2 + \alpha_T\} \left[\frac{n_S - 3n_T - 1}{2} \right] \right. \\
&\quad \left. + \frac{\xi_V^2}{2} \{1 - n_S - 3n_T\} \right) \ln^2\left(\frac{k}{k_*}\right) + \dots, \\
\xi_V^2(k) &= \xi_V^2 - \frac{1}{2} (\kappa_S - 4\kappa_T + 4n_T^2 \{n_S - n_T - 1\}) \ln\left(\frac{k}{k_*}\right) \\
&\quad + \frac{1}{4} \left(\xi_V^2 \{16n_T^2 + 9n_T [n_S - 3n_T - 1] + [n_S - 3n_T - 1]^2 + 2\xi_V^2\} \right) \ln^2\left(\frac{k}{k_*}\right) + \dots, \\
\sigma_V^3(k) &= \sigma_V^3 + \sigma_V^3 (1 - n_S) \ln\left(\frac{k}{k_*}\right) + \frac{\sigma_V^3}{4} \left(30n_T^2 + 20n_T [n_S - 3n_T - 1] + \xi_V^2 + 2[n_S - 3n_T - 1]^2 \right) \ln^2\left(\frac{k}{k_*}\right) + \dots
\end{aligned} \tag{32}$$

where at the pivot scale $k = k_*$ the slow roll parameters are defined as follows:

$$\epsilon_V = \frac{M_P^2}{2} \left(\frac{V'}{V} \right)^2, \quad \eta_V = M_P^2 \left(\frac{V''}{V} \right), \quad \xi_V^2 = M_P^4 \left(\frac{V'V'''}{V^2} \right), \quad \sigma_V^3 = M_P^6 \left(\frac{V'^2 V''''}{V^3} \right). \tag{33}$$

Additionally, the appearance of very mild running (α_S, α_T) and running of the running (κ_S, κ_T) of the spectrum might have implications for the *Primordial black hole* formation [61].

Once the higher order radiative corrections are incorporated due to the presence of running in the parameterization of the power spectrum, then the inflationary observables can be expressed as:

$$P_S(k_*) = [1 - (2\mathcal{C}_E + 1)\epsilon_V + \mathcal{C}_E\eta_V]^2 \frac{V}{24\pi^2 M_{PL}^4 \epsilon_V}, \quad P_T(k_*) = [1 - (\mathcal{C}_E + 1)\epsilon_V]^2 \frac{2V}{3\pi^2 M_{PL}^4}, \tag{34}$$

$$n_S - 1 \approx (2\eta_V - 6\epsilon_V) - 2\mathcal{C}_E \xi_V^2 + \frac{2}{3} \eta_V^2 + 2(8\mathcal{C}_E + 3)\epsilon_V^2 + 2\epsilon_V \eta_V \left(6\mathcal{C}_E + \frac{7}{3} \right) - 4\mathcal{C}_E (\mathcal{C}_E + 1) \xi_V^2 \epsilon_V + 2\mathcal{C}_E^2 \eta_V \xi_V^2, \tag{35}$$

$$n_T \approx -2\epsilon_V + 2 \left(2\mathcal{C}_E + \frac{5}{3} \right) \epsilon_V \eta_V - 2 \left(4\mathcal{C}_E + \frac{13}{3} \right) \epsilon_V^2, \tag{36}$$

$$r(k_*) = 16\epsilon_V \frac{[1 - (\mathcal{C}_E + 1)\epsilon_V]^2}{[1 - (2\mathcal{C}_E + 1)\epsilon_V + \mathcal{C}_E\eta_V]^2} \approx 16\epsilon_V [1 + 2\mathcal{C}_E(\epsilon_V - \eta_V)], \tag{37}$$

$$\begin{aligned}
\alpha_S \approx & (16\eta_V \epsilon_V - 24\epsilon_V^2 - 2\xi_V^2) - 2\mathcal{C}_E (4\epsilon_V \xi_V^2 - \eta_V \xi_V^2 - \sigma_V^3) + \frac{4}{3} \eta_V (2\eta_V \epsilon_V - \xi_V^2) + 4(8\mathcal{C}_E + 3)\epsilon_V (4\epsilon_V^2 - 2\eta_V \epsilon_V) \\
& - 4\mathcal{C}_E (\mathcal{C}_E + 1) [\epsilon_V (4\epsilon_V \xi_V^2 - \eta_V \xi_V^2 - \sigma_V^3) + \xi_V^2 (4\epsilon_V^2 - 2\eta_V \epsilon_V)] + 2\mathcal{C}_E^2 \xi_V^2 (2\eta_V \epsilon_V - \xi_V^2) \\
& + 2\mathcal{C}_E^2 \eta_V (4\epsilon_V \xi_V^2 - \eta_V \xi_V^2 - \sigma_V^3),
\end{aligned} \tag{38}$$

$$\alpha_T \approx (4\eta_V \epsilon_V - 8\epsilon_V^2) + 2 \left(2\mathcal{C}_E + \frac{5}{3} \right) [\epsilon_V (2\eta_V \epsilon_V - \xi_V^2) + \eta_V (4\epsilon_V^2 - 2\eta_V \epsilon_V)] - 4 \left(4\mathcal{C}_E + \frac{13}{3} \right) \epsilon_V (4\epsilon_V^2 - 2\eta_V \epsilon_V), \tag{39}$$

$$\begin{aligned}
\kappa_S \approx & 192\epsilon_V^2\eta_V - 192\epsilon_V^3 + 2\sigma_V^3 - 24\epsilon_V\xi_V^2 + 2\eta_V\xi_V^2 - 32\eta_V^2\epsilon_V - 8C_E [\epsilon_V(4\epsilon_V\xi_V^2 - \eta_V\xi_V^2 - \sigma_V^3) + \xi_V^2(4\epsilon_V^2 - 2\eta_V\epsilon_V)] \\
& + 2C_E [\eta_V(4\epsilon_V\xi_V^2 - \eta_V\xi_V^2 - \sigma_V^3) + \xi_V^2(2\eta_V\epsilon_V - \xi_V^2)] + 4C_E\sigma_V^3(3\epsilon_V - \eta_V) + \frac{4}{3}(2\eta_V\epsilon_V - \xi_V^2)^2 \\
& + \frac{4}{3}\eta_V [2\eta_V(4\epsilon_V^2 - 2\eta_V\epsilon_V) + 2\epsilon_V(2\eta_V\epsilon_V - \xi_V^2) - (4\epsilon_V\xi_V^2 - \eta_V\xi_V^2 - \sigma_V^3)] \\
& + 4(8C_E + 3)(4\epsilon_V^2 - 2\eta_V\epsilon_V)^2 + 16(8C_E + 3)\epsilon_V [(2\epsilon_V - \eta_V)(4\epsilon_V^2 - 2\eta_V\epsilon_V) - \epsilon_V(2\eta_V\epsilon_V - \xi_V^2)] \\
& + 4 \left(6C_E + \frac{7}{3}\right) (2\eta_V\epsilon_V - \xi_V^2)(4\epsilon_V^2 - 2\eta_V\epsilon_V) + 2 \left(6C_E + \frac{7}{3}\right) \epsilon_V [2(2\eta_V\epsilon_V - \xi_V^2)\epsilon_V + 2\eta_V(4\epsilon_V^2 - 2\eta_V\epsilon_V) \\
& - (4\epsilon_V\xi_V^2 - \eta_V\xi_V^2 - \sigma_V^3)] - 4C_E(C_E + 1)(4\epsilon_V^2 - 2\eta_V\epsilon_V)(4\epsilon_V\xi_V^2 - \eta_V\xi_V^2 - \sigma_V^3) \\
& - 4C_E(C_E + 1)\epsilon_V [(4\epsilon_V - \eta_V)(4\epsilon_V\xi_V^2 - \eta_V\xi_V^2 - \sigma_V^3) + (16\epsilon_V^2 + \xi_V^2 - 10\eta_V\epsilon_V)\xi_V^2 - 2\sigma_V^3(3\epsilon_V - \eta_V)] \\
& - 4C_E(C_E + 1) [(4\epsilon_V\xi_V^2 - \eta_V\xi_V^2 - \sigma_V^3)(4\epsilon_V^2 - 2\eta_V\epsilon_V) + 2\xi_V^2((4\epsilon_V - \eta_V)[4\epsilon_V^2 - 2\eta_V\epsilon_V] - \epsilon_V[2\eta_V\epsilon_V - \xi_V^2])] \\
& + 2C_E^2[(4\epsilon_V\xi_V^2 - \eta_V\xi_V^2 - \sigma_V^3)(2\eta_V\epsilon_V - \xi_V^2) + \xi_V^2(2\eta_V(4\epsilon_V^2 - 2\eta_V\epsilon_V) + 2\epsilon_V(2\eta_V\epsilon_V - \xi_V^2) - [4\epsilon_V\xi_V^2 - \eta_V\xi_V^2 \\
& - \sigma_V^3])] + 2C_E^2[(2\eta_V\epsilon_V - \xi_V^2)(4\epsilon_V\xi_V^2 - \eta_V\xi_V^2 - \sigma_V^3) + \eta_V[(4\epsilon_V - \eta_V)[4\epsilon_V\xi_V^2 - \eta_V\xi_V^2 - \sigma_V^3] + \xi_V^2[16\epsilon_V^2 + \xi_V^2 \\
& - 10\eta_V\epsilon_V] - 2\sigma_V^3[3\epsilon_V - \eta_V])],
\end{aligned} \tag{40}$$

$$\begin{aligned}
\kappa_T \approx & 56\eta_V\epsilon_V^2 - 64\epsilon_V^3 - 8\eta_V^2\epsilon_V - 4\epsilon_V\xi_V^2 + 2 \left(2C_E + \frac{5}{3}\right) [(2\eta_V\epsilon_V - \xi_V^2)(4\epsilon_V^2 - 2\eta_V\epsilon_V) \\
& + \epsilon_V(2\eta_V[4\epsilon_V^2 - 2\eta_V\epsilon_V] + 2\epsilon_V[2\eta_V\epsilon_V - \xi_V^2] - [4\epsilon_V\xi_V^2 - \eta_V\xi_V^2 - \sigma_V^3]) \\
& + \eta_V(8\epsilon_V[4\epsilon_V^2 - 2\eta_V\epsilon_V] - 2\eta_V[4\epsilon_V^2 - 2\eta_V\epsilon_V] - 2\epsilon_V[2\eta_V\epsilon_V - \xi_V^2])] \\
& - 4 \left(4C_E + \frac{13}{3}\right) [(4\epsilon_V^2 - 2\eta_V\epsilon_V)^2 + \epsilon_V((8\epsilon_V - 2\eta_V)[4\epsilon_V^2 - \epsilon_V] - 2\epsilon_V[2\eta_V\epsilon_V - \xi_V^2])].
\end{aligned} \tag{41}$$

where $C_E = 4(\ln 2 + \gamma_E) - 5$ with $\gamma_E = 0.5772$ is the *Euler-Mascheroni constant* originating in the expansion

of the gamma function. For details discussion on these aspects see Refs [43].

-
- [1] P. A. R. Ade *et al.* [Planck Collaboration], [arXiv:1303.5082](#) [astro-ph.CO].
- [2] G. Hinshaw *et al.* [WMAP Collaboration], [arXiv:1212.5226](#) [astro-ph.CO].
- [3] A. Mazumdar and J. Rocher, Phys. Rept. **497**, 85 (2011) [[arXiv:1001.0993](#) [hep-ph]].
- [4] M. Pospelov and J. Pradler, Ann. Rev. Nucl. Part. Sci. **60**, 539 (2010) [[arXiv:1011.1054](#) [hep-ph]].
- [5] P. A. R. Ade *et al.* [Planck Collaboration], [arXiv:1303.5076](#) [astro-ph.CO].
- [6] M. Cicoli and A. Mazumdar, JCAP **1009**, 025 (2010) [[arXiv:1005.5076](#) [hep-th]]. M. Cicoli and A. Mazumdar, Phys. Rev. D **83**, 063527 (2011) [[arXiv:1010.0941](#) [hep-th]].
- [7] S. Angus, J. P. Conlon, U. Haisch and A. J. Powell, [arXiv:1305.4128](#) [hep-ph].
- [8] K. Enqvist and A. Mazumdar, Phys. Rept. **380**, 99 (2003) [[arXiv:hep-ph/0209244](#)].
- [9] A. R. Liddle, A. Mazumdar and F. E. Schunck, Phys. Rev. D **58**, 061301 (1998) [[arXiv:astro-ph/9804177](#)].
- [10] R. Allahverdi, K. Enqvist, J. Garcia-Bellido and A. Mazumdar, Phys. Rev. Lett. **97**, 191304 (2006) [[arXiv:hep-ph/0605035](#)].
- [11] R. Allahverdi, K. Enqvist, J. Garcia-Bellido, A. Jokinen and A. Mazumdar, JCAP **0706**, 019 (2007) [[arXiv:hep-ph/0610134](#)].
- [12] R. Allahverdi, A. Kusenko and A. Mazumdar, JCAP **0707**, 018 (2007) [[arXiv:hep-ph/0608138](#)].
- [13] L. Wang, E. Pukartas and A. Mazumdar, [[arXiv:1303.5351](#) [hep-ph]].
- [14] A. Mazumdar, S. Nadathur and P. Stephens, Phys. Rev. D **85**, 045001 (2012) [[arXiv:1105.0430](#) [hep-th]].
- [15] S. Choudhury and S. Pal, JCAP **1204**, 018 (2012) [[arXiv:1111.3441](#) [hep-ph]].
- [16] A. Chatterjee and A. Mazumdar, JCAP **1109**, 009 (2011) [[arXiv:1103.5758](#) [hep-ph]].
- [17] C. S. Aulakh and I. Garg, Phys. Rev. D **86**, 065001 (2012) [[arXiv:1201.0519](#) [hep-ph]].
- [18] S. Downes, B. Dutta and K. Sinha, [[arXiv:1106.2266](#) [hep-th]]. R. Allahverdi, S. Downes and B. Dutta, [[arXiv:1106.5004](#) [hep-th]].
- [19] J. C. Bueno Sanchez, K. Dimopoulos and D. H. Lyth, JCAP **0701**, 015 (2007) [[arXiv:hep-ph/0608299](#)].
- [20] K. Enqvist, A. Mazumdar and P. Stephens, JCAP **1006**, 020 (2010) [[arXiv:1004.3724](#) [hep-ph]]. S. Hotchkiss, A. Mazumdar and S. Nadathur, JCAP **1106**, 002 (2011) [[arXiv:1101.6046](#) [astro-ph.CO]].
- [21] R. K. Jain, P. Chingangbam, J. -O. Gong, L. Sriramkumar and T. Souradeep, JCAP **0901**, 009 (2009) [[arXiv:0809.3915](#) [astro-ph]]. R. K. Jain, P. Chingangbam, L. Sriramkumar and T. Souradeep, Phys. Rev. D **82**, 023509 (2010) [[arXiv:0904.2518](#) [astro-ph.CO]].
- [22] S. Hotchkiss, A. Mazumdar and S. Nadathur, JCAP **1202**, 008 (2012) [[arXiv:1110.5389](#) [astro-ph.CO]].
- [23] A. Ashoorioon, P. S. B. Dev and A. Mazumdar, [[arXiv:1211.4678](#) [hep-th]].

- [24] A. D. Linde, Phys. Lett. B **259**, 38 (1991); Phys. Rev. D **49** (1994) 748 [[arXiv:astro-ph/9307002](#)].
- [25] G. R. Dvali, Q. Shafi and R. K. Schaefer, Phys. Rev. Lett. **73**, 1886 (1994) [[arXiv:hep-ph/9406319](#)].
- [26] C. Pallis and Q. Shafi, [arXiv:1304.5202](#) [hep-ph].
- [27] S. Unnikrishnan and V. Sahni, [arXiv:1305.5260](#) [astro-ph.CO].
- [28] C. Boehm, J. Da Silva, A. Mazumdar and E. Pukartas, Phys. Rev. D **87**, 023529 (2013) [[arXiv:1205.2815](#) [hep-ph]].
- [29] R. Allahverdi, B. Dutta and A. Mazumdar, Phys. Rev. D **75**, 075018 (2007) [[arXiv:hep-ph/0702112](#) [hep-ph]].
- [30] M. R. Douglas and S. Kachru, Rev. Mod. Phys. **79**, 733 (2007) [[arXiv:hep-th/0610102](#)].
- [31] R. Allahverdi, B. Dutta and A. Mazumdar, Phys. Rev. D **78** 063507 (2008) [[arXiv:0806.4557](#) [hep-ph]].
- [32] K. Enqvist, L. Mether, S. Nurmi, JCAP **0711**, 014 (2007).
- [33] Z. Lalak and K. Turzyski, Phys. Lett. B **659**, 669 (2008)
- [34] S. Kasuya and M. Kawasaki, Phys. Rev. D **74**, 063507 (2006) [[arXiv:hep-ph/0606123](#)].
- [35] M. Dine, L. Randall and S. D. Thomas, Phys. Rev. Lett. **75**, 398 (1995) [[arXiv:hep-ph/9503303](#)].
- [36] M. Dine, L. Randall and S. D. Thomas, Nucl. Phys. B **458**, 291 (1996) [[arXiv:hep-ph/9507453](#)].
- [37] M. Berg, M. Haack and B. Kors, JHEP **0511**, 030 (2005) [[arXiv:hep-th/0508043](#)].
- [38] H. P. Nilles, Phys. Rept. **110**, 1 (1984).
- [39] <https://twiki.cern.ch/twiki/bin/view/AtlasPublic/SupersymmetryPublicResults>
- [40] <https://twiki.cern.ch/twiki/bin/view/CMSPublic/SUSYSMSSummaryPlots8TeV>
- [41] D. H. Lyth and A. R. Liddle, “The primordial density perturbation: Cosmology, inflation and the origin of structure,” Cambridge, UK: Cambridge Univ. Pr. (2009) 497 p.
- [42] A. R. Liddle, P. Parsons and J. D. Barrow, Phys. Rev. D **50**, 7222 (1994) [[astro-ph/9408015](#)].
- [43] R. Easther and H. Peiris, JCAP **0609**, 010 (2006) [[arXiv:astro-ph/0604214](#)].
- [44] A. Lewis and S. Bridle, Phys. Rev. D **66** 103511 (2002) [[arXiv:astro-ph/0205436](#)]. For update see the link: <http://camb.info/>.
- [45] N. D. Birrell and P. C. W. Davies, Quantum Fields in Curved Space, Cambridge University Press, 1984.
- [46] Andrew R. Liddle and David H. Lyth, Cosmological Inflation and Large-Scale Structure, Cambridge University Press, 2000.
- [47] P. A. R. Ade *et al.* [Planck Collaboration], [arXiv:1303.5075](#) [astro-ph.CO].
- [48] A. R. Liddle and S. M. Leach, Phys. Rev. D **68**, 103503 (2003) [[astro-ph/0305263](#)].
- [49] C. P. Burgess, R. Easther, A. Mazumdar, D. F. Mota and T. Multamaki, JHEP **0505**, 067 (2005) [[arXiv:hep-th/0501125](#)].
- [50] R. Allahverdi, A. Ferrantelli, J. Garcia-Bellido and A. Mazumdar, Phys. Rev. D **83**, 123507 (2011) [[arXiv:1103.2123](#) [hep-ph]].
- [51] G. Jungman, M. Kamionkowski and K. Griest, Phys. Rept. **267**, 195 (1996) [[hep-ph/9506380](#)].
- [52] R. Allahverdi, B. Dutta and Y. Santoso, Phys. Rev. D **82**, 035012 (2010) [[arXiv:1004.2741](#) [hep-ph]].
- [53] J. R. Ellis, J. E. Kim and D. V. Nanopoulos, Phys. Lett. B **145** (1984) 181.
- [54] M. Bolz, A. Brandenburg and W. Buchmuller, Nucl. Phys. B **606** (2001) 518 [Erratum-ibid. B **790** (2008) 336] [[arXiv:hep-ph/0012052](#)].
- [55] A. L. Maroto and A. Mazumdar, Phys. Rev. Lett. **84**, 1655 (2000) [[arXiv:hep-ph/9904206](#)]. R. Kallosh, L. Kofman, A. D. Linde and A. Van Proeyen, Phys. Rev. D **61**, 103503 (2000) [[hep-th/9907124](#)]. H. P. Nilles, M. Peloso and L. Sorbo, Phys. Rev. Lett. **87**, 051302 (2001) [[hep-ph/0102264](#)]. H. P. Nilles, M. Peloso and L. Sorbo, JHEP **0104**, 004 (2001) [[hep-th/0103202](#)].
- [56] T. Moroi, [arXiv:hep-ph/9503210](#).
- [57] R. Allahverdi and A. Mazumdar, JCAP **0610**, 008 (2006) [[hep-ph/0512227](#)].
- [58] R. Allahverdi, A. R. Frey and A. Mazumdar, Phys. Rev. D **76** 026001 (2007) [[arXiv:hep-th/0701233](#)].
- [59] Planck Collaboration (total dataset and cosmology products), See: <http://irsa.ipac.caltech.edu/data/Planck>, <http://pla.esac.esa.int/pla/aio/planckProducts.html>.
- [60] W. Hu, N. Sugiyama and J. Silk, Nature **386**, 37 (1997) [[astro-ph/9604166](#)].
- [61] M. Drees and E. Erfani, JCAP **1201**, 035 (2012) [[arXiv:1110.6052](#) [astro-ph.CO]]. M. Drees and E. Erfani, JCAP **1104**, 005 (2011) [[arXiv:1102.2340](#) [hep-ph]].